

Full load estimation of an offshore wind turbine based on SCADA and accelerometer data

N Noppe^{1,2}, A Iliopoulos³, W Weijtjens^{1,2} and C Devriendt^{1,2}

¹ Acoustics and Vibrations Research Group (AVRG), Vrije Universiteit Brussel, Pleinlaan 2, B1050 Brussels, Belgium

² Offshore Wind Infrastructure lab (OWI-lab), Belgium

³ Department of Mechanics of Materials and Constructions, Vrije Universiteit Brussel, Pleinlaan 2, B1050 Brussels, Belgium

E-mail: nymfa.noppe@avrg.be

Abstract. As offshore wind farms (OWFs) grow older, the optimal use of the actual fatigue lifetime of an offshore wind turbine (OWT) and predominantly its foundation will get more important. In case of OWTs, both quasi-static wind/thrust loads and dynamic loads, as induced by turbulence, waves and the turbine's dynamics, contribute to its fatigue life progression. To estimate the remaining useful life of an OWT, the stresses acting on the fatigue critical locations within the structure should be monitored continuously. Unfortunately, in case of the most common monopile foundations these locations are often situated below sea-level and near the mud line and thus difficult or even impossible to access for existing OWTs. Actual strain measurements taken at accessible locations above the sea level show a correlation between thrust load and several SCADA parameters. Therefore a model is created to estimate the thrust load using SCADA data and strain measurements. Afterwards the thrust load acting on the OWT is estimated using the created model and SCADA data only. From this model the quasi static loads on the foundation can be estimated over the lifetime of the OWT. To estimate the contribution of the dynamic loads a modal decomposition and expansion based virtual sensing technique is applied. This method only uses acceleration measurements recorded at accessible locations on the tower. Superimposing both contributions leads to a so-called multi-band virtual sensing. The result is a method that allows to estimate the strain history at any location on the foundation and thus the full load, being a combination of both quasi-static and dynamic loads, acting on the entire structure. This approach is validated using data from an operating Belgian OWF. An initial good match between measured and predicted strains for a short period of time proves the concept.

1. Introduction

Fatigue life is an important design consideration for the most common monopile foundation of offshore wind turbines (OWTs). The current practice for life time assessment is based on conservative design assumptions and simplifications due to uncertainties in earlier designs. This conservatism potentially leads to under-estimation of the actual fatigue life. On the contrary, a continuous monitoring system with the ability to assess the stress history and consequently the fatigue life consumption of individual turbines can best support wind farm's operation and maintenance (O&M) actions as well as end-of-life decisions [1, 2, 3]. Such a monitoring system requires the installation of (strain) sensors for direct strain measurement at fatigue critical locations. However, two big limitations exist in the case of OWTs in an offshore



wind farm (OWF): unfeasibility of sensor installation at fatigue hotspots beneath the water level (e.g. mudline) and high cost of sensor placement on all turbines of the OWF. The aforementioned limitations establish the need for implementation of virtual sensing techniques for fatigue assessment.

[4] illustrates a successful virtual sensing technique by combining strain measurements and acceleration measurements. Unfortunately, strain gauges are known to become unreliable over time. Hence, this paper introduces an alternative strategy combining 1s SCADA data, thus eliminating the need for strain measurements, and accelerations from reliable accelerometers installed at accessible locations of the structure above sea level. As the strain data driven approach requires installation of additional strain gauges on every turbine to be monitored, expansion to the entire OWF is considered cost-ineffective. The SCADA driven approach on the other hand can be easily expanded to the entire OWF, considering that SCADA data is available for every turbine without the need of installing additional sensors.

A conceptual illustration of the followed data-driven approach is given in Figure 1. First more information about the measurement campaign and additional data is given in Section 2. Section 3 explains the estimation of thrust load, using 1s SCADA data only. To obtain this estimation a model is created using actual strain measurements and SCADA data. The thrust load results in a quasi-static strain prediction at fatigue critical locations, as described in Section 4.1. Additionally, this hybrid approach should not be limited to only thrust loads but should also be capable to capture any structural dynamics caused by resonant motion or wave loading. Therefore acceleration measurements are used, as explained in Section 4.2. By combining both quasi-static and dynamic contributions, a multi-band virtual sensing (Section 4.3) is accomplished. Preliminary results are shown in Section 5. Subsequently Section 6 concludes this paper and Section 7 elaborates on future work.

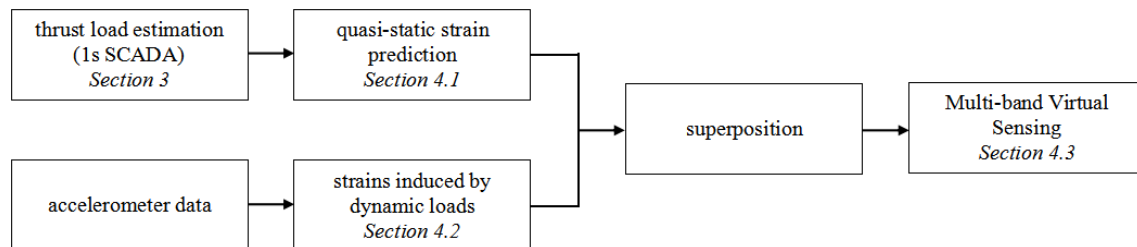


Figure 1. Conceptual illustration of the proposed virtual sensing technique

2. Measurement campaign

This contribution uses accelerometer and strain data obtained from a measurement campaign performed at the Belwind wind farm, consisting of 55 Vestas 3MW V90 turbines installed on monopile foundations. The wind farm is located in the North Sea, 46 km off the Belgian coast. One turbine, situated in the middle of the farm, was instrumented with accelerometers in the beginning of 2012 and with strain gauges in September 2014. The campaign is currently still ongoing.

Acceleration measurements are taken at 4 levels using a total of 10 accelerometers. Eight accelerometers (two per level) capture the vibrations in the X-Y direction and the two additional accelerometers at the highest level (tower top) are utilized to identify torsional vibrations in the tower. The locations are chosen based on the convenience of sensor mounting, such as the vicinity of platforms. Moreover four fiber Bragg grating (FBG) sensors at the Tower/Transition Piece interface have been installed. Figure 2 gives an overview of the instrumented OWT at the Belwind farm. The acceleration data of the upper levels will be used in order to predict the

dynamic strains at the lower levels and ultimately at critical and inaccessible hotspot locations. The strain data can be transformed into actual thrust forces, which will be compared with the modeled ones utilised for quasi-static strain prediction.

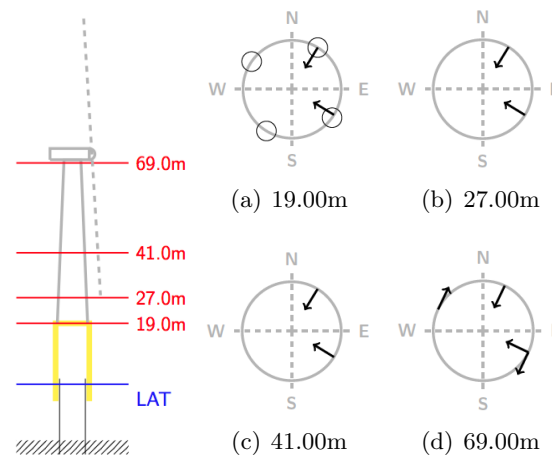


Figure 2. Instrumentation of BBC01 wind turbine at the Belwind farm. The circles in (a) indicate the presence of a Fiber Bragg Grating strain sensor; the arrows in (a-d) indicate the presence of an accelerometer.

In addition to the acceleration and strain measurements, a subset of measurements recorded by the Supervisory Control And Data Acquisition (SCADA) system is available as well. The main purpose of the SCADA system is to monitor and control plants, for which reason it records continuously. Although SCADA data has the advantage of being available by default, it needs to be handled with care: there is no guarantee that the sensors used to measure the acquired parameters are accurately calibrated over the entire lifetime of the turbine. For instance, the wind speed is measured by an anemometer installed behind the rotor, which is known for being unreliable [5]. In the available subset (of both, the 1s data set and the 10 min data set), measurements for wind speed, wind direction, power production, blade pitch angle, rotor speed and yaw angle can be found.

From the continuous data acquisition and by applying state of the art operational modal analysis techniques that have been fully automated [6, 7, 8], the natural frequencies, the modeshapes and the damping ratios of the OWT are obtained. At a next stage, a finite element model (FEM) that resembles the actual tower/foundation components of the OWT is built-up using a sequence of pipe elements. The cylindrical geometry of the structure as well as the wall thickness of each section is based on as-designed values, since the (preferred) as-built dimensions are not available for this turbine. The FEM is tuned in order to match the modal properties obtained experimentally. For more details about the tuning of the structure, the reader is referred to [9].

3. Load modeling using SCADA

Being able to predict the thrust load using 1s SCADA data would have several advantages. For instance a SCADA system is installed on every turbine. Therefore 1s SCADA data is in theory available for each turbine.

According to [10], it is possible to calculate the thrust load with Equation (1), where ρ is the air density, U the wind speed, R the rotor radius, C_T the thrust coefficient, θ the blade pitch angle and ω the rotor speed.

$$T = \frac{1}{2} \rho U^2 \pi R^2 C_T(\theta, U, \omega) \quad (1)$$

In this equation, all parameters are measured by the SCADA system except for the air density and the thrust coefficient. The air density is considered constant during the current analysis, however its influence on the thrust load will be studied in future work. This coefficient depends on the design of the turbine and is considered to be dependent on the blade pitch angle and the tip speed ratio [10]. Since the tip speed ratio can be calculated using the wind speed and the rotor speed, the thrust coefficient should be dependent on SCADA parameters only: blade pitch angle, wind speed and rotor speed. Hence a model to estimate the thrust load can be created based on SCADA data. In this contribution, a data-driven model will be created, which will approximate the model given by Equation (1). Once such a model is found, it will be valid for every turbine of the same type.

The thrust load is modeled using the 10 minute average SCADA data and 10 minute average strain measurements. The actual bending moment, and thus the actual thrust load, is calculated from these strain measurements. Both the actual thrust load and the SCADA data for a period of 4 months is used. Figure 3 shows the averaged measured thrust load, divided into 3 groups based on the operational state of the turbine.

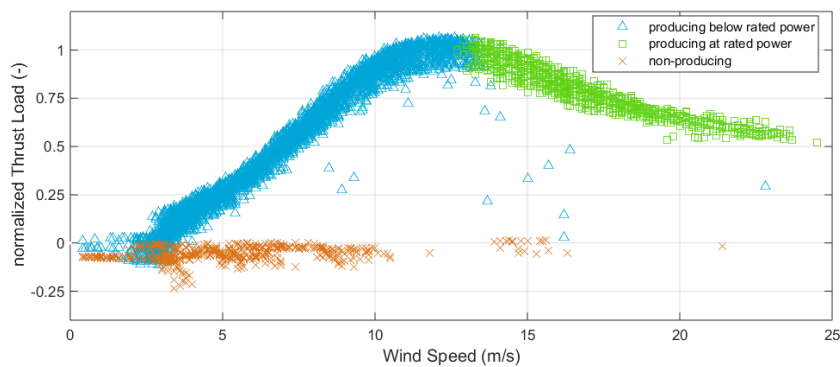


Figure 3. 10 min averages of thrust load, calculated from measured strains, vs wind speed. The data points are divided into 3 regimes: non-producing, producing below rated power and producing at rated power.

The decision of which input parameters should be used to create the model is based on Equation (1). The wind speed, blade pitch angle and rotor speed are the parameters available in the SCADA subset and thus these shall be used as input parameters. However, given the unreliability of the anemometer [5], which provides the wind speed for the SCADA data set, the wind speed should be excluded as much as possible from the input parameter sets. When the turbine is producing below rated power, the produced power can replace the wind speed as input parameter since both are directly related to each other by the warranted power curve. If the turbine is producing at rated power, the changes in blade pitch angle are correlated with the changes in wind speed. The aforementioned is summarized in Table 1.

Table 1. For every regime, a neural network is trained with a different input parameter set

	Non-producing	Producing below rated power	Producing at rated power
blade pitch angle	x	△	□
rotor speed	x	△	□
wind speed	x		
produced power		△	

For each of the three regimes the data set is split randomly into a training (60%), a validation (20%) and a testing (20%) set. To train a neural network with the resulting training set, the default Matlab functions are used. This means the training dataset is randomly split up a second time into training (70%), validation (15%) and test data (15%). A feedforward neural network with one hidden layer is trained with the remaining training data, based on the Levenberg-Marquardt algorithm. The transfer function for the hidden layer is a tan-sigmoid transfer function; for the output layer it is a linear transfer function. The training stops when the validation error failed to decrease for six iterations. This procedure is repeated for a number of neurons starting from 1 to 20. Based on the root mean squared error of the initial testing set, the optimal number of neurons is chosen.

Table 2 gives the resulting normalized mean absolute error and normalized root mean squared error for the validation set of each regime.

Table 2. The normalized Mean Absolute Error (MAE) and normalized Root Mean Squared Error (RMSE) of each neural network on validation data set

	Non-producing	Producing below rated power	Producing at rated power
normalized MAE	0,0242	0,0312	0,0226
normalized RMSE	0,0326	0,0407	0,0327

Finally, the resulting model to estimate the thrust load combines the three neural networks. Figure 4(a) shows the resulting modeled thrust load for 10 min averages of SCADA data, together with the measured thrust load. Figure 4(b) shows the normalized error between measured and modeled thrust load for the three regimes. The data shown covers a period of 4 months, including the training, testing and validation sets.

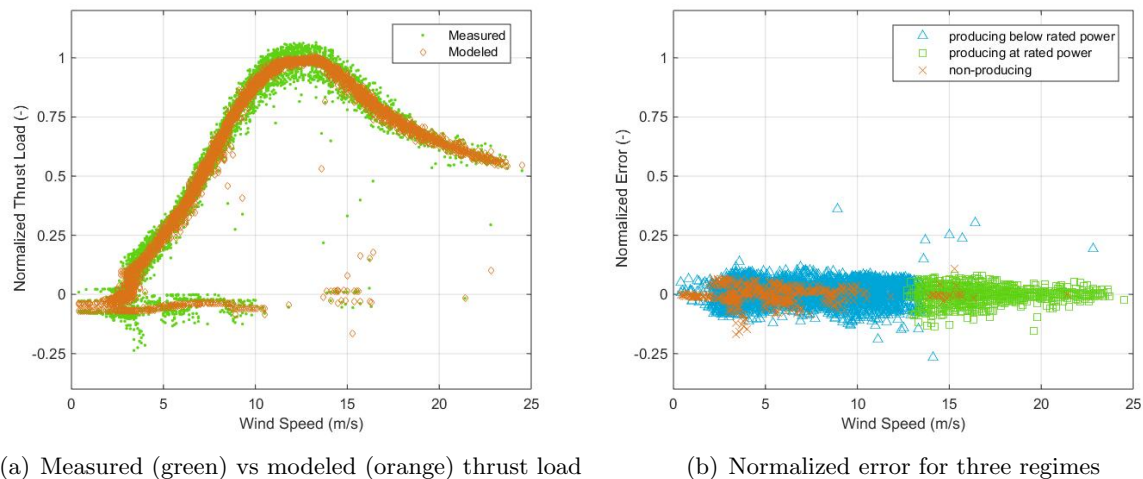


Figure 4. Resulting modeled thrust load based on 10 min SCADA parameters compared to 10 min averages of measured thrust load: (a) shows the normalized values for thrust load, (b) shows the normalized error. Data representing a period of 4 months is shown, including training, testing and validation sets.

For fatigue monitoring the thrust load is required at a higher sampling rate than 10 minute averages. However, the found model can also take 1s SCADA as input to predict the quasi-static thrust load at a higher sampling rate. It is this estimation that will be used for virtual sensing. This will be discussed in the next sections.

4. Virtual Sensing

Virtual sensing allows to estimate the strains at any fatigue hotspot without the necessity of prior sensor installation on the hotspot itself. As the structure has a different behavior when excited due to a static load in comparison to excitation due to a dynamic load, both types of loads are treated differently. This distinction is made based on the frequency spectrum of the loads acting on an OWT, as shown in Figure 5. The quasi-static thrust load can be estimated using 1s SCADA data. Unfortunately, with a 1 second sampling rate only loads up to 0.5Hz can be captured. Loads with higher frequencies such as the rotor dynamic and turbulence induced loads are thus not captured by SCADA parameters. Moreover, wave and current loads have no relation to SCADA and can thus also not be captured using a SCADA model. Both wave and high frequent loads are combined as dynamic loads. To capture these dynamic loads accelerometers are installed at easily accessible locations.

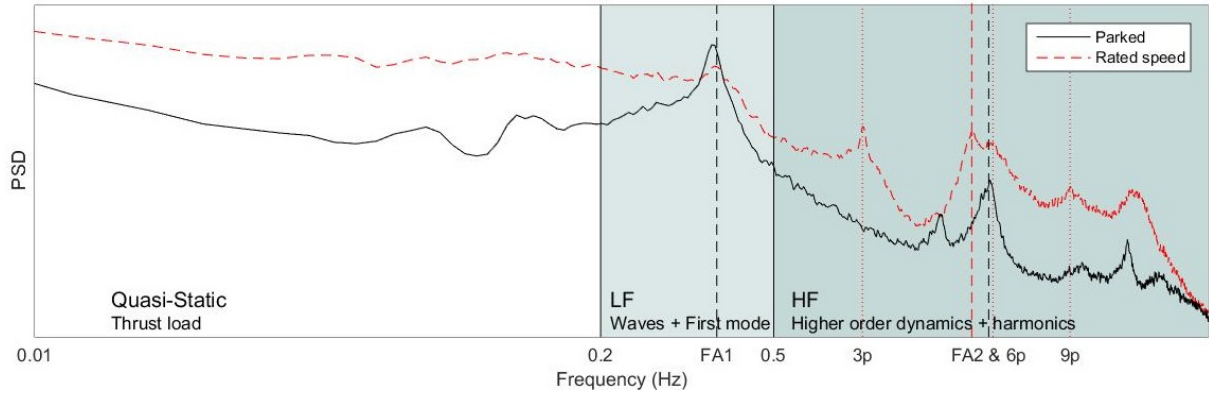


Figure 5. Frequency spectrum of the measured loads acting on an operating OWT. The quasi-static variations are captured by the 1s SCADA data, while the dynamic variations are captured by the accelerometer data.

4.1. SCADA-driven quasi-static strain prediction

At very low frequencies situated well below the first eigenfrequency and below the site-specific wave peak frequency, a.k.a. quasi-static region of frequencies, the induced strains are caused by thrust loading. Under thrust load the strain distribution of the turbine differs from the strain distribution of the lowest structural mode. This implies the need for different strain mode shape components to represent the thrust load induced strains. Figure 6 demonstrates this aforementioned difference in strain distribution and motivates the use of static strain mode shape components for the prediction of quasi-static strains. Equation (2) is used to predict the quasi-static strains:

$$\varepsilon_{\mathbf{p}}^{\text{QS}}(t) = \phi_{\varepsilon_{\mathbf{p}}}^{\text{QS}} \frac{T(t)}{T_{\text{ref}}} \quad \forall t \quad (2)$$

where $\phi_{\varepsilon_{\mathbf{p}}}^{\text{QS}} \in \mathbb{R}^{n_p \times 1}$ is the quasi-static strain distribution at the n_p DOFs which correspond to the virtual sensor locations p , $T(t)$ is the modeled, using SCADA, thrust load for each time instance t and T_{ref} is the reference thrust load which is exerted as a static load at the tower top of the tuned FEM in order to obtain the quasi-static strain distribution.

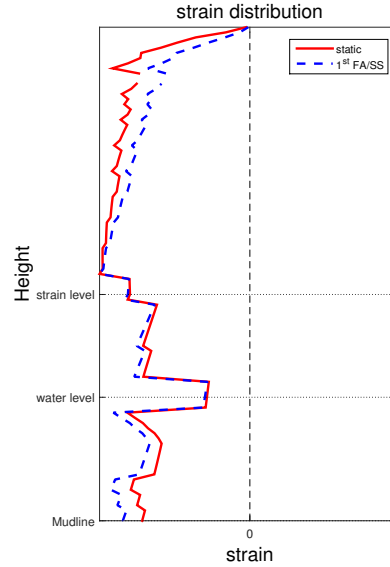


Figure 6. Static strain distribution (red full line) and 1st FA/SS strain mode shape (blue dashed line) from mudline to tower top level

4.2. Dynamic strain prediction

The modal decomposition and expansion based virtual sensing technique [11, 12] is used for dynamic strain prediction. The theoretical background of this approach has been extensively presented in previous works of the authors [13, 14, 9, 15, 16] and is repeated briefly hereafter. Firstly, a modal decomposition of the measured accelerations is performed resulting in the estimation of the "acceleration" modal coordinates $\mathbf{q}(t)$. Since strain is related to modal displacements, the integration of these modal coordinates is required. In this work, a double integration in the Laplace domain was used resulting in the $\frac{1}{s^2}$ operation. At a next step, a change from Laplace domain to the time domain for continuous strain prediction is achieved using the inverse Laplace transformation, $\mathcal{L}^{-1}\{\bullet\}$. Finally, the estimated time domain displacement modal coordinates are multiplied with the corresponding strain mode shape components derived numerically from a tuned finite element model. Doing so, the prediction of dynamic strain in any virtual location is established. Equation (3) summarizes the discussed process.

$$\epsilon_{\mathbf{p}}^{\mathbf{D}}(t) = \Phi_{\epsilon p} \mathcal{L}^{-1} \left\{ \frac{1}{s^2} \mathcal{L} \{ \mathbf{q}(t) \} \right\} \quad (3)$$

where $\Phi_{\epsilon p} \in \mathbb{R}^{n_p \times n}$ are strain mode shapes of the n considered modes at the n_p DOFs which correspond to the virtual sensor locations p , $\mathbf{q}(t) = \{q_1(t), q_2(t), \dots, q_n(t)\}^T$ are the modal coordinates that quantify the participation of each mode and $\mathcal{L}\{\bullet\}$, $\mathcal{L}^{-1}\{\bullet\}$ are the Laplace and inverse Laplace operations respectively.

The dynamic frequency band is subdivided in two parts as seen in Figure 5. The first part captures the lower frequency turbine dynamics including the first structural mode (0.2 Hz up to 0.5 Hz) and the second part (0.5 Hz -) captures all the remaining dynamics and modal behavior of the structure. The reason for this subdivision is the benefit from the optimal use of the best performing sensors in each dynamic frequency band. For example, sensors near the top of the turbine are very valuable for assessing the first order motion, while sensors closer to the bottom are nearly insensitive to this first order motion and they barely measure above the noise floor.

For higher modes in the high-frequent dynamic band multiple modes and multiple sensors are necessary in order to optimally capture the dynamics.

Not only the quasi-static load, but also the dynamics of the OWT in non-power producing state differ from those in power producing state. Specifically, in the case of the non-producing turbine, even one mode ($n=1$) and one sensor can be sufficient enough to fully describe its dynamic behavior as the spectrum is mainly dominated by the first mode. On the contrary, in the case of the producing turbine a linear combination of multiple modes is considered.

4.3. Multi-band virtual sensing

Both the quasi-static and the dynamic strain prediction contribute to the fatigue of an OWT. Therefore a superposition of both quasi-static and dynamic contributions is made, leading to a prediction of the entire strain time history. This is called multi-band virtual sensing and is summarized by Equation (4).

$$\varepsilon_p(t) = \varepsilon_p^{QS}(t) + \varepsilon_p^D(t) \quad (4)$$

5. Results and discussion

In Figure 7.(a-b) indicative results of SCADA-driven quasi-static strain response ε_p^{QS} and dynamic strain response ε_p^D are shown. Moreover, a superposition of these contributions (ε_p) is also given in Figure 7.(c). These results are obtained for an operating OWT at rated speed. It is nicely observed that the predicted strains adequately match the measured strains both in the sub-bands and in the entire band of interest.

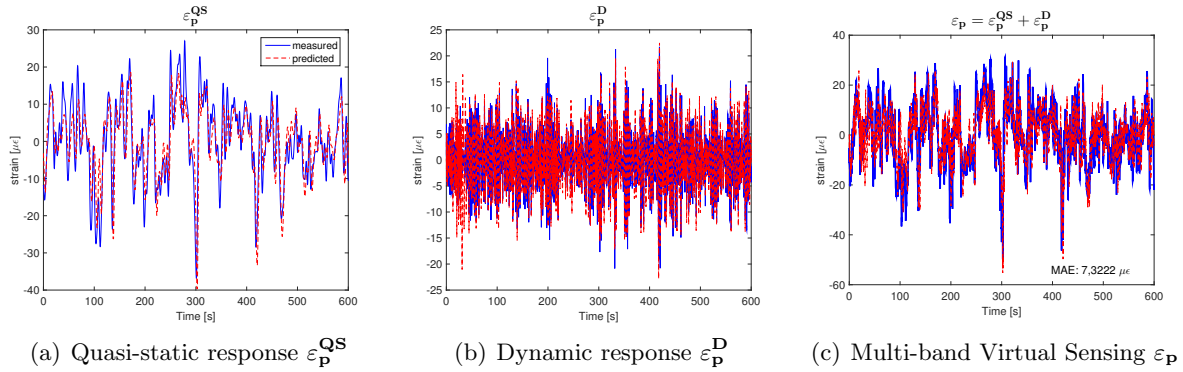


Figure 7. SCADA-driven quasi-static strain response and acceleration-driven dynamic strain response superimposed resulting in the so-called multi-band virtual sensing. The mean absolute error obtained for this example is shown in (c). The blue full line is the actual measured signal and the red dashed line is the predicted signal with the proposed technique. The example dataset corresponds to normal operating condition at rated rotor speed of the OWT.

The performance of the technique is also demonstrated by a couple of examples in Figure 8, where various operational states are represented. A good match seems to be found between the predicted and the measured strains, both in terms of amplitude and in terms of temporal evolution. This is reflected in both time and frequency domain. In case of the two examples shown first (a-c) and (d-f), an important contribution of the quasi-static thrust load can be observed. This is also reflected in the frequency domain, as the spectral density for frequencies lower than 0,2 Hz is comparable to the spectral density of the first mode. However for the third example (g-i), the thrust load seems to contribute very little. This indicates that for low winds,

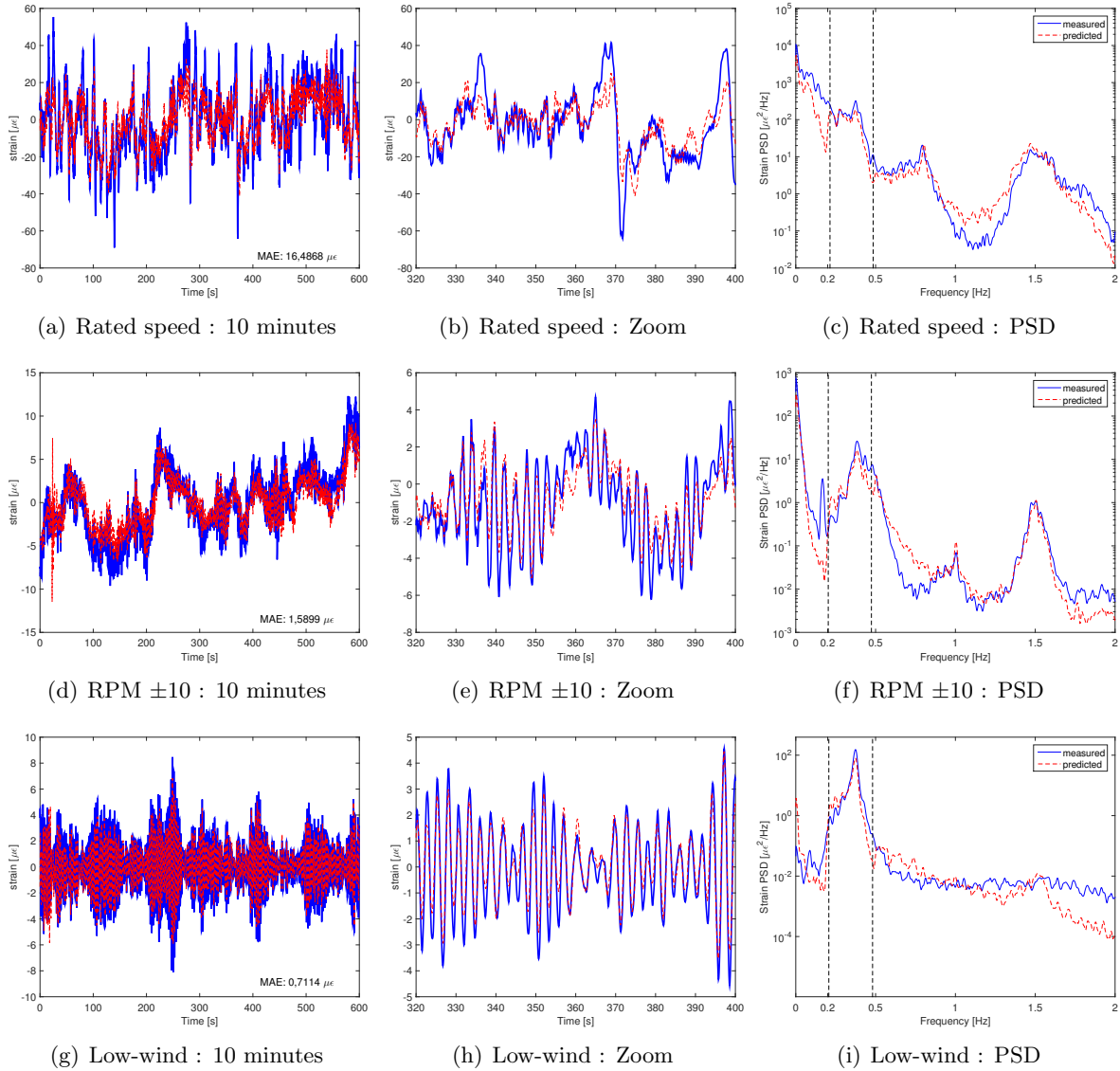


Figure 8. Multi-band virtual sensing validated for a variety of operational cases. The blue full line represents the actual measured signal and the red dashed line the predicted signal with the proposed technique. The mean absolute error for each example is shown in (a,d,g).

the dynamics are dominant, whereas for higher winds the thrust load will have a contribution equally important. The same observation can be made in Figure 5. Moreover, the frequency spectrum for frequencies higher than 0,2Hz (ie the dynamic part) indicates a dominance of the first mode. This justifies the use of only one mode to estimate the dynamic behavior of the turbine.

To compare these results to the ones obtained with the strain data driven approach, as explained in [17], the mean absolute error (MAE) is calculated for the given examples. The values for MAE are promising for the second and third example (d,g), 1,5899 and 0,7114 respectively, but an improvement is needed based on the values obtained for the first example (a) and the example shown in Figure 7, 16,4868 and 7,3222 respectively, both representing production at rated speed. The frequency spectra indicates the importance of the quasi-static part is higher in this case than for non-producing or producing below rated speed. Therefore it's most likely an improvement

of the thrust model will influence the result considerably.

However the results obtained based on 10 min averages shown in Section 3 showed little difference between the three regimes. This rises the question if a model fitted based on 10 min averages is applicable on 1s data.

6. Conclusion

This paper introduced and validated an approach to estimate the contribution of both quasi-static and dynamic loads to the stresses acting on fatigue hotspots of an offshore wind turbine (OWT). This is done by using 1s SCADA data and additional accelerometer data, measured at easily accessible locations of OWT. To estimate the quasi-static thrust loads, a model is created with 10 min SCADA data and 10 min averages of additional strain measurements. Based on the thrust estimation a quasi-static strain response can be predicted. The strain response of dynamic loads is predicted using a modal decomposition and expansion based virtual sensing technique based on acceleration measurements. By superposing both the quasi-static and dynamic contribution a full strain history of an OWT is obtained. The results shown in this contribution are promising. A good match between predicted and measured strains can be found, but some examples indicate an improvement of the model to estimate the thrust load is still needed.

7. Future Work

Although the followed approach gives promising results, some of these indicate an improvement of the estimation of the quasi-static thrust load might be necessary. Therefore a closer look can be taken to the input data set used for the training of the model. Not only the choice of input parameters or possible filters should be questioned, but a comparison between the performance of a model trained with 10min SCADA and the performance of one trained with 1s SCADA data is needed as well. Furthermore other techniques to create such a model, e.g. regression trees or linear modeling need to be considered. Once the model is improved and the approach is validated on short term for normal operation regimes, a short term validation in case of a start/stop event will be done. Afterwards the technique will be validated for longer periods of several days up to months.

As explained in the paper, the model obtained to estimate the thrust load should be valid for every turbine of the same type. Therefore a cross-validation of the model on another turbine of the same type will be performed.

Once an accurate stress history can be obtained for the full structure, this will result in consumed fatigue life. However for wind farm owners the fatigue life of the entire OWF is important, not the fatigue life of only one OWT. Hence this fatigue assessment done for one OWT should be extrapolated over the entire OWF.

Acknowledgements

This research has been performed in the framework of the Offshore Wind Infrastructure Project (<http://www.owi-lab.be>) and the O&O Parkwind project. The authors also acknowledge the financial support by the Agency for innovation by Science and Technology (IWT) and the Research Fund-Flanders (FWO). The authors gratefully thank the people of Parkwind and Belwind for their continued support throughout this project.

References

- [1] Yang W, Tavner P J, Crabtree C J, Feng Y and Qiu Y 2014 *Wind Energy* **17** 673–693
- [2] Haddad G, Sandborn P and Pecht M 2014 *Wind Energy* **17** 775–791

- [3] Griffith D T, Yoder N C, Resor B, White J and Paquette J 2014 *Wind Energy* **17** 1737–1751
- [4] Iliopoulos A, Weijtjens W, Van Hemelrijck D and Devriendt C Fatigue assessment of offshore wind turbines on monopile foundations using virtual sensing , under review for *Wind Energy*
- [5] Noppe N, Weijtjens W and Devriendt C 2015 Reliable empirical analysis of effects of turbulent air in an operating wind farm based on unreliable scada data poster presented at EAWE PhD Seminar, 22-25 Sept 2015, Stuttgart
- [6] Devriendt C, Magalhães F, Weijtjens W, De Sitter G, Cunha Á and Guillaume P 2014 *Structural Health Monitoring* **13** 644–659
- [7] Weijtjens W, De Sitter G, Devriendt C and Guillaume P 2014 Automated transmissibility based operational modal analysis for continuous monitoring in the presence of harmonics *Proceedings of the 9th International Conference on Structural Dynamics, EURODYN* ed Cunha Á, Ribeiro G and Müller G pp 2231–2238
- [8] El-Kafafy M, Devriendt C, Weijtjens W, De Sitter G and Guillaume P 2014 Evaluating different automated operational modal analysis techniques for the continuous monitoring of offshore wind turbines *Dynamics of Civil Structures, Volume 4* (Springer International Publishing) pp 313–329
- [9] Iliopoulos A, Shirzadeh R, Weijtjens W, Guillaume P, Van Hemelrijck D and Devriendt C 2016 *Mechanical Systems and Signal Processing* **68** 84–104
- [10] Baudisch R 2012 *Structural Health Monitoring of Offshore Wind Turbines* Master's thesis DTU
- [11] Avitabile P and Pingle P 2012 *Shock and Vibration* **19** 765 – 785 ISSN 0888-3270 URL <http://www.hindawi.com/journals/sv/2012/408919/abs/>
- [12] Baghersad J, Niezrecki C and Avitabile P 2015 *Mechanical Systems and Signal Processing* **6263** 284 – 295 ISSN 0888-3270 URL <http://www.sciencedirect.com/science/article/pii/S0888327015001478>
- [13] Iliopoulos A, Weijtjens W, Van Hemelrijck D and Devriendt C 2016 Full-field strain prediction applied to an offshore wind turbine *Model Validation and Uncertainty Quantification, Volume 3* (Springer) pp 349–357
- [14] Maes K, Iliopoulos A, Weijtjens W, Devriendt C and Lombaert G 2016 *Mechanical Systems and Signal Processing* **76** **77** 592 – 611 ISSN 0888 - 3270 URL <http://www.sciencedirect.com/science/article/pii/S0888327016000066>
- [15] Iliopoulos A N, Weijtjens W, Van Hemelrijck D and Devriendt C 2015 *Journal of Physics: Conference Series* **628** 012108 URL <http://stacks.iop.org/1742-6596/628/i=1/a=012108>
- [16] Iliopoulos A, Weijtjens W, Van Hemelrijck D and Devriendt C 2015 Long-term prediction of dynamic responses on an offshore wind turbine using a virtual sensor approach *Proceedings of the 10th International Workshop on Structural Health Monitoring 2015: System Reliability for Verification and Implementation, p. 2809-2816, Stanford, CA-USA*
- [17] Iliopoulos A, Weijtjens W, Van Hemelrijck D and Devriendt C 2016 Full-field strain prediction applied to an offshore wind turbine *Proceedings of IMAC XXXIV, Orlando, FL, USA*